

Quantitative Study of the Effect of Coverage on the Hybridization Efficiency of Surface-Bound DNA Nanostructures

Elham Mirmomtaz,^{†,‡,§,◆} Matteo Castronovo,^{†,‡,⊥,¶,◆} Christian Grunwald,^{†,¶,▽,◆}
Fouzia Bano,^{†,¶} Denis Scaini,^{†,¶,¶} Ali A. Ensafi,[§] Giacinto Scoles,^{*,†,‡,⊥}
and Loredana Casalini^{†,⊥}

ELETTRA, Sincrotrone Trieste S.C.p.A., S.S. 14 Km 163.5 Basovizza, 34012 Trieste, Italy, International Center for Theoretical Physics (ICTP), Strada Costiera 11, 34014, Trieste, Italy, Department of Chemistry, Isfahan University of Technology (IUT), Isfahan, 84156, Iran, Scuola Internazionale Superiore di Studi Avanzati (SISSA), 34014 Trieste, Italy, Italian Institute of Technology (IIT) - SISSA Unit, 34014 Trieste, Italy, and Physics Department, University of Trieste, Via Valerio 2, 34127 Trieste, Italy

Received September 8, 2008

ABSTRACT

We demonstrate that, contrary to current understanding, the density of probe molecules is not responsible for the lack of hybridization in high density single-stranded DNA (ss-DNA) self-assembled monolayers (SAMs). To this end, we use nanografting to fabricate well packed ss-DNA nanopatches within a “carpet matrix” SAM of inert thiols on gold surfaces. The DNA surface density is varied by changing the “writing” parameters, for example, tip speed, and number of scan lines. Since ss-DNA is 50 times more flexible than ds-DNA, hybridization leads to a transition to a “standing up” phase. Therefore, accurate height and compressibility measurements of the nanopatches before and after hybridization allow reliable, sensitive, and label-free detection of hybridization. Side-by-side comparison of self-assembled and nanografted DNA-monolayers shows that the latter, while denser than the former, display higher hybridization efficiencies.

There are two main challenges in the development of new analytical methods for the detection of DNA hybridization. The first lies in reducing the minimum amount of DNA that can be directly (label- and PCR-free) detected. In this context, nanopatterned detection devices are to be preferred because when signal levels do not depend on the pattern size, they require a smaller number of molecules to reach “saturation”. If reliable detection of a small number of hybridizations

could be achieved, it would allow for the rapid detection of single cell RNA pools and would be quite useful in forensic, neuron classification, and other applications.^{1–3} The second challenge is represented by the need of quantitative analysis for gene expression profiles that, using current technology, is limited by our partial knowledge of the hybridization efficiency in all surface-based detection schemes.^{1,4–8}

Many PCR-dependent methods based on, for instance, electrochemical,^{9,10} surface plasmon resonance,¹¹ and fluorescence detection have been proposed.^{4,12,13} Among these, the most common are microarrays in which labeling target molecules and feature sizes larger than 10 μm are necessary. It is important to realize that a 10 μm spot provides space for up to 25 million DNA molecules, which, in addition to the problem of quantitatively introducing fluorescence labels, makes it clear why PCR-free detection of low copy number (e.g., <1000) RNA sequences is a difficult task.^{4,11}

Furthermore, the detection of small amounts of noncoding RNAs is especially interesting since often these molecules are involved in gene expression regulation, for example, in

* To whom correspondence should be addressed. E-mail: scoles@sisssa.it.
Phone: +39 040 3758689. Fax: +39 040 3758565.

[†] ELETTRA, Sincrotrone Trieste S.C.p.A.

[‡] International Center for Theoretical Physics (ICTP).

[§] Isfahan University of Technology (IUT).

[¶] Scuola Internazionale Superiore di Studi Avanzati (SISSA).

[⊥] Italian Institute of Technology (IIT) - SISSA Unit.

[¶] University of Trieste.

[◆] Present address: CBM S.r.l - Cluster in Molecular Biomedicine, S.S. 14 Km 163.5, Basovizza, 34012 Trieste, Italy.

[▽] Present address: Johann Wolfgang Goethe-Universität Frankfurt am Main, Institute of Biochemistry, Biocenter Max-von-Laue-Strasse 9 D-60438 Frankfurt, Germany.

[◆] These authors contributed equally to the work.

the cell division cycle.^{14,15} Abnormal regulation of the cell division process results in cancer and can be biochemically tracked down to malfunction (mutation) of individual proteins. Therefore capturing and quantifying of low amounts of RNAs from a few or even a single cell is not only desirable for biological basic research, but also for cancer diagnostics and, possibly, therapeutics.^{1,3,5,6}

Self-assembled monolayers (SAMs) of DNA chemisorbed, typically, on gold (111) surfaces have been intensively studied as model systems as they allow investigation of hybridization reactions in surface tethered, spatially constrained DNA films. Although different DNA surface densities are easily accessible by changing concentrations and incubation times, inconsistent values have been reported for the saturation density of surface tethered DNA molecules.^{16–20}

In this work, we aim at advancing the state of the art in this area in two ways. First, building on the nanografting work of G.Y. Liu and co-workers,^{21,22} we demonstrate that a very low number of target DNA molecules can be reliably detected using height and/or compressibility measurements of DNA nanostructures. Second, by varying the number of scanning lines during nanografting over the area in which desired DNA nanostructure is being assembled, we show that we can control the nanoscale DNA surface density. This, coupled to in situ side-by-side comparison of hybridization of self-assembled and nanografted DNA-monolayers, has allowed us to prove that the probe density alone is not responsible for the lack of hybridization in high density ss-DNA SAMs as reported in the literature by at least two groups.^{16,18} Since we have independent evidence that a nanografted monolayer patch is better ordered than a spontaneously adsorbed monolayer made with the same molecules, we are led to the conclusion that it is the intrinsic lack of order (instead of the density) that is the determining factor in strongly hindering the hybridization of maximum density SAMs. Our findings provide valuable biophysical insight on the organization and hybridization of short DNA fragments tethered on surfaces with clear implications for the fabrication and operation of DNA nanoarrays. To simplify the rest of the paper we would like to introduce a new term that would identify an adsorbed monolayer, in which the assembly has been assisted by an external agent, as a nanografting assembled monolayers (NAM).

Nanografting, first introduced by Liu in 1997,²³ is today a well-established technique for nanopatterning of SAMs,²⁴ (for a review, see ref 25; for a theoretical modeling study, see ref 26). Our starting point is a flat gold (111) surface covered by a protective SAM of oligo-ethylene-glycol (OEG) modified thiols ($\text{HS}-(\text{CH}_2)_{11}-(\text{OCH}_2\text{CH}_2)_3-\text{OH}$). During DNA nanografting an AFM tip is scanned in a solution containing thiolated DNA at a relatively high load (few tens of nN) over the desired nanopatch area. Due to tip-induced mechanical perturbations, the OEG molecules in the protective SAM locally exchange with thiolated DNA molecules present in solution and the so fabricated nanopatch can be imaged after resetting the value of the perpendicular force load to the smallest possible, still detectable, value. In their

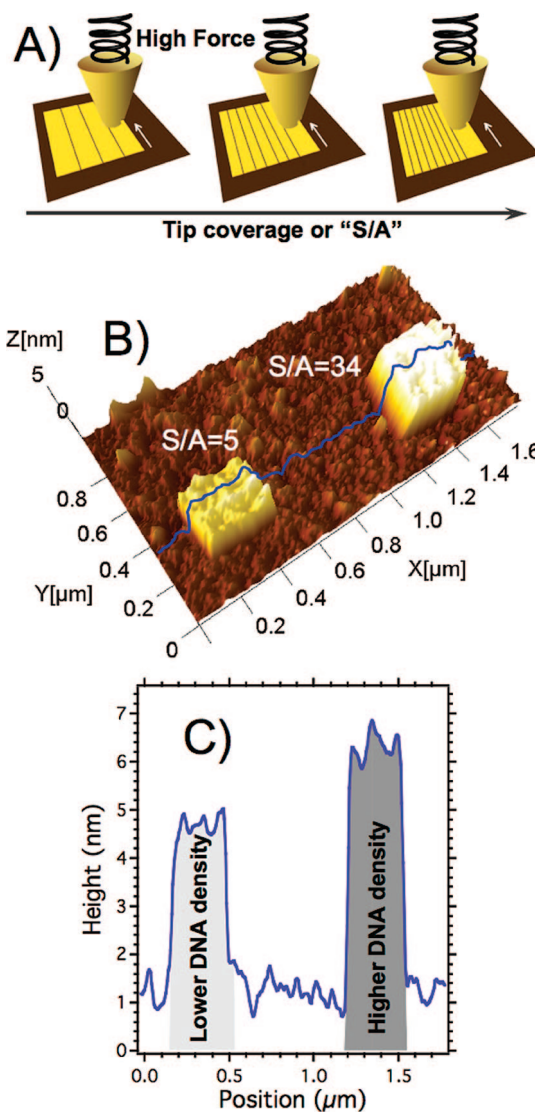


Figure 1. (A) Illustration of the definition of the nanografted line density (S/A parameter, see text). (B) AFM topographic image of two ssDNA nanopatches (NAM) obtained with $S/A = 5$ (left) and $S/A = 34$ (right) written into a bioresistant OEG-SAM before the hybridization. (C) A profile of the NAM in B (see the blue line) indicates that the conformation of ssDNA molecules inside NAMs significantly depends upon S/A parameter.

pioneering work about DNA nanografting, Liu and co-workers have varied DNA concentration, scan-speed of the AFM tip, loading force and scan-line density during nanografting, to show that nanografted DNA patches of standing-up molecules could be fabricated.²²

We have systematically studied the increased height, by using the height of the OEG SAM as a reference (i.e., about 1.5 nm from the gold(111) surface²⁷) of the ss-DNA nanopatches at constant scan area, loading force, and DNA concentration. Varying the number of scanning lines during the nanografting process, that is, by grafting over the same area more than once, we find increasing heights for ss-DNA-nanopatches written at higher line overlap (see Figure 1).

To compare DNA-nanopatches of different sizes and to learn about the density of DNA as a function of the number of times any given area is nanografted over, it is useful to

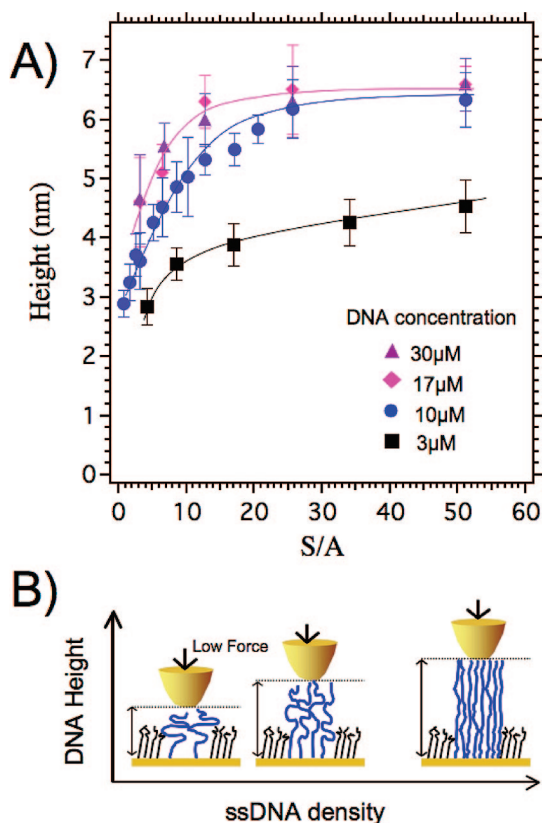


Figure 2. (A) Height of ss-DNA NAM nanografted within an OEG SAM as a function of the S/A line density. During grafting ss-DNA concentration of 3.0 (black squares), 10.0 (blue dots), 17.0 (violet triangles), and 30.0 (pink rhombuses) μM have been tested (solid lines were drawn to guide the eyes through the curves). Here colored lines are shown only just to drive the eyes along the curves. (B) A scheme depicts our interpretation for which the increase of NAMs height is due to an increase of the density of DNA molecules.

introduce a line density parameter “ S/A ” where S is the scanned area and A is the actual area of the final patch. $S/A = R \cdot N/L$ in which R is the width of the tip at the point of contact with the surface, and N/L is the number of scan lines (in the slow scan direction) divided by the length of the patch L (in the same direction). For example, for $S/A = 1$ the nanografted lines do not overlap with each other, while for $S/A = 3$ each spot in the nanopatch has been nanografted 3 times over, as shown in the cartoon in Figure 1A.

In Figure 1B, we show two ss-DNA nanopatches fabricated at low and high S/A number, respectively. The associated topography profiles (Figure 1C) show that with increased S/A numbers the height of the nanopatch increases, to indicate that more DNA-molecules are grafted into the same nanoarea. These findings are extended in Figure 2A, where ss-DNA nanopatches heights are plotted, for a wide range of S/A values, at different DNA concentrations in a buffer solution. With the exception of the lowest concentration (that needs higher values of S/A to saturate) in Figure 2A, we can see that all height plots reach the same saturation value, between 6 and 7 nm, which is close to the length of the fully extended conformation of an 18-mer sequence such as the one used here. In the S/A range between 1 and 15, the height of the DNA-nanopatches is highly sensitive

to the chosen S/A number provided the probe concentration during nanografting is high enough (e.g., greater than 10 μM).

The fact that when grafting additional ss-DNA molecules into the patch the height of the latter increases is certainly not surprising because the height of a ss-DNA NAM, made of standing-up, thiolated, molecules, is in fact affected by the repulsive van der Waals overlap forces and/or the electrostatic repulsion between the DNA oligomers which make them to stretch in the vertical (unconstrained) direction at higher densities (see scheme in Figure 2B). What is interesting and somewhat of a surprise to us is the fact that our results clearly establish that the maximum height reached by NAMs is much larger than that reached by a maximum density SAM (see below). We can only speculate at this point that during nanografting the structures that we create are undergoing a sort of tip-induced local annealing (or perhaps combing) getting more dense and much less entangled at the same time, up to the limit that can be calculated for a structure with the same height of fully stretched ss-DNA molecules. This result is to be contrasted with the (likely correct) observations reported in the literature for ss-DNA SAMs, according to which spontaneous self-assembly is associated with a certain degree of molecular entanglement.²⁰ If disorder/entanglement would be present in our flexible ss-DNA nanostructures, we should expect that full utilization of space would be hindered and that sizable portions of the molecule would not be vertical, resulting in a patch height lower than the nominal, fully stretched, molecular height. We will come back to the crucial issue of molecular order in nanografted DNA structures later in this paper, giving more direct evidence for our hypothesis.

After establishing the correspondence between the height of the nanopatches and the S/A density parameter, we investigated how the system behaves upon hybridization. We found that, in the low S/A regime, after hybridization, the height of the DNA-nanopatches increases significantly, due to the much higher stiffness of ds-DNA with respect to ss-DNA (see Figure 3). Measurements of cross-reactivity of a DNA target molecule to noncomplementary ss-DNA nanostructures (data not shown) confirmed that the height increase in the low density regime is selectively associated with a matching complementary ss-DNA target molecule. Indeed, when exposing the DNA nanostructures of a few different sequences to DNA molecules complementary only to one of them, no changes in height of ss-DNA-nanopatches were observed for all the noncomplementary cases.

As expected, in the high S/A regime, in which the height of the nanopatches has already reached saturation, no change in height is recognized upon hybridization (see Figure 3). It follows that in the high S/A regime it is not possible to know whether or not hybridization occurs using height measurements, because no further change in height can be expected once the ss-DNA inside the nanopatches is organized in its fully extended conformation. Compressibility measurements (e.g., height measurements versus up to moderately elevated loading forces) offer a reliable way for checking if hybridization also occurs in the high S/A regime.

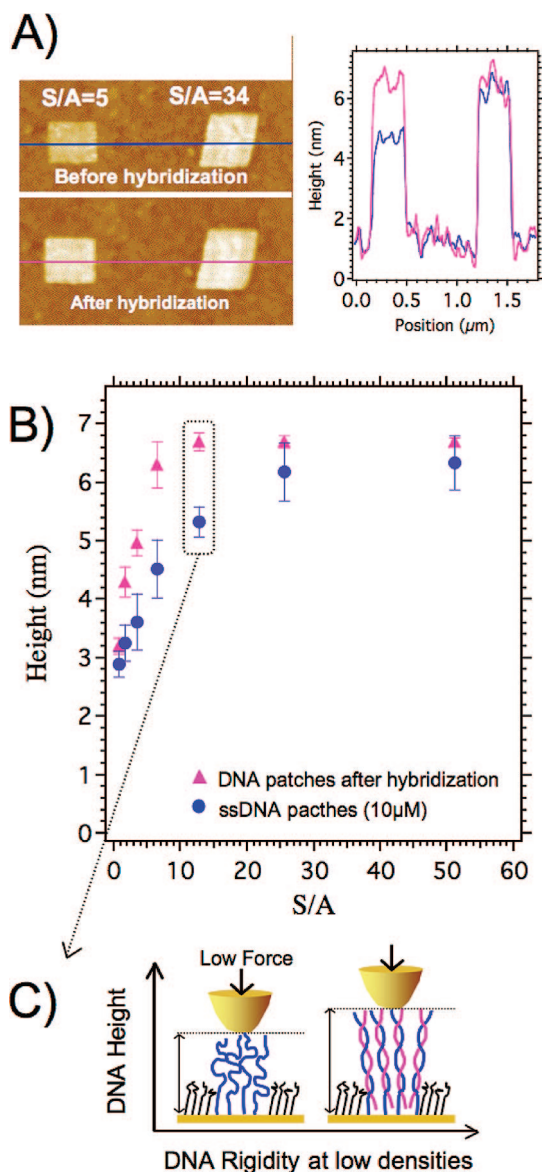


Figure 3. (A) On the left, DNA NAMs ($S/A = 5$ and $S/A = 34$) relative to Figure 1A,B, before and after hybridization. On the right, height profiles show the height change due to hybridization. The height increase only for NAM at $S/A = 5$. (B) Relative height of NAM in the $10 \mu\text{M}$ case relative to Figure 2A. The relative height of DNA NAM within an OEG SAM is measured before (blue dots) and after hybridization (pink triangles). The plots indicate that in the low packing regime ($SN \leq 20$) the height of the NAMs increases sensitively upon hybridization. (C) A scheme depicts our interpretation of the height increase of the DNA patch in the low S/A range (e.g., $S/A = 10$) upon hybridization.

The height-to-load response of 3 NAMs made, respectively, with ss-DNA, ds-DNA, and ds-DNA produced by in situ full hybridization of ss-DNA-nanopatches, was investigated at $S/A = 50$. The results are summarized in Figure 4A revealing three important findings: (1) the elastic response of DNA-nanopatches before (in blue) and after hybridization (in pink) differs sufficiently to allow for easy identification; (2) ds-DNA is almost incompressible with forces below 16 nN, which is consistent with the fact that the persistence length of ds-DNA is 50 times larger than that of ss-DNA;

(3) the stiff mechanical response of the in situ hybridized DNA nanostructure (in pink) is almost identical to that of the nanografted ds-DNA-nanopatch (in black). These results are schematized in the cartoon of Figure 4B.

From the changes in compressibility we conclude that in nanografted patches also in the high S/A (density) regime hybridization occurs even if the heights before and after hybridization are, of course, the same. However, a quantitative determination of the hybridization efficiency of our highly dense patches is not yet possible from the presented data. Toward this end, we studied the compressibility behavior of nanopatches of mixed ss-DNA and ds-DNA composition. In particular, we grafted a mixture containing 50% ss-DNA and 50% ds-DNA (brown filled squares in Figure 4C) and a mixture with 20% ds-DNA and 80% ss-DNA (green filled circles in Figure 4C). While in the latter case data points are in between the compressibility plots of ss-DNA and ds-DNA of Figure 4A, the former series of data were almost indistinguishable from the 100% grafted ds-DNA, proving that the hybridization efficiency in our nanografted patches is at least 50%, that is, much higher than the value of 10% reported in the literature for the high-density DNA SAMs.¹⁸

To give a direct proof that it is the sterical hindrance due to the disorder in the film that inhibits hybridization in DNA SAMs and that our NAM patches are more ordered, following what was done previously by other groups we directly compared our nanopatches with the DNA SAM. Since both Tarlov and Georgiadis groups, who extensively studied DNA SAMs, found the hybridization reaction to be very inefficient at high monolayer coverages, we used their protocols^{16,18} to produce a high density SAM, into which we created DNA patches by nanografting. In this way we use the same detection technique, that is, topography height, to compare DNA SAMs and NAM patches excluding any possible influence of the detection technique on the contrasting results. Therefore, we nanografted a DNA sequence into a SAM of the same DNA sequence, obtained, according to the Tarlov protocol, from prolonged immersion (more than 24 h) of the gold substrate into a highly concentrated (microMolar) solution of ssDNA molecules. In Figure 5 an AFM topography image and relative profiles of this “autografted” ssDNA patch is shown (Figure 5B), together with an image and profile of a patch of the same density ($S/A = 5$) nanografted into a TOEG SAM (Figure 5A). To establish the absolute height of all four systems compared here, the height of the high density SAM surrounding the patch of Figure 5B is then measured by creating a squared “hole” in the SAM by nanoshaving, as shown in Figure 5C. While the height of the ssDNA NAM patch does not change whether it is embedded into a TOEG SAM or into a DNA carpet (Figure 5A,B), the height of a NAM patch, which is not even saturated, is found to be more than twice the height of a maximum density ssDNA SAM. This result is clearly suggesting that in our DNA nanopatches not only the density but also the degree of order is larger than in SAMs. Moreover, we verified that the height of the high density ssDNA SAM does not change upon hybridization; detailed

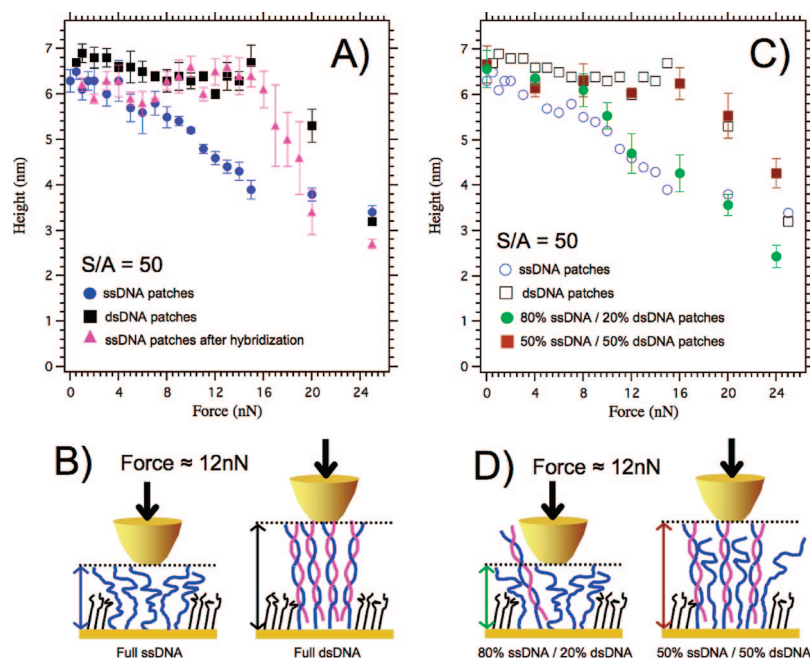


Figure 4. (A) Relative height of high density DNA NAMs ($S/A = 50$) measured as a function of the load applied by the AFM tip (compressibility curves). The mechanical resistance of a DNA NAM hybridized in situ (pink triangles) is very distinguishable from the one relative to the same NAM before hybridization (blue dots), but is very similar to the behavior of a NAM of ds-DNA, that is, nanografted after hybridization in solution (black squares). (B) A scheme depicts the result shown in panel A for ssDNA NAMs and dsDNA NAMs under an applied force of 12 nN. (C) Compressibility curves of high density DNA NAMs ($S/A = 50$) with mixed composition, that is, 80% ssDNA/20% dsDNA (filled green circles) and 50% ssDNA/50% dsDNA (filled brown squares), are compared to the compressibility curves of panel A relative to fully ssDNA NAMs (now reported with open blue circles) and fully dsDNA NAMs (now reported with open black squares). This observation indicates that the hybridization efficiency within highly dense ss-DNA NAM is certainly higher than the value, that is, about 10%, reported in the literature for high density ss-DNA SAM. (D) A scheme depicts the result shown in panel B for mixed DNA NAMs under an applied force of 12 nN.

studies on the hybridization of DNA SAMs of different densities will be shown in a separate paper.²⁸

We have demonstrated that when combining height and elastic compressibility measurements it is possible to detect hybridization of nanostructured DNA. In particular, we have used nanografting to control the density and improve the molecular packing in ss-DNA nanoassemblies, demonstrating that even in very dense NAMs the efficiency of hybridization is larger than 50% hereby demonstrating that molecular density cannot be the sole source for the inefficient ($<10\%$) hybridization in high coverage SAMs.

Very recently the group of Belcher et al. reported on hybridization detection of ss-DNA nanostructures produced by dip-pen nanolithography by means of kelvin-probe-microscopy.²⁹ While the detection method was shown to work efficiently on the nanoscale, the proposed nanodevices lack a detailed knowledge of the conformational state of the molecules in the patches. By using nanografting in combination with height profile measurements, we have provided for the first time a method to control systematically the surface coverage of DNA on the nanoscale while at the same time to detect quantitatively the hybridization efficiency of ss-DNA nanostructures.

Nanografted DNA monolayers hybridize differently than DNA SAMs. First of all NAMs can achieve heights not achievable by SAMs made using the same oligonucleotides. Furthermore, their asymptotic high density height corresponds to the fully extended conformation of their DNA

molecules which likely reflects the lack of entanglement for the densely packed surface tethered DNA molecules. Finally at all coverage values explored (far inside the height saturation regime), we could not identify a range of densities in which hybridization would not steadily increase.

Hybridization-induced rearrangement of DNA probe molecules tethered to a solid interface was previously described by Tarlov and co-workers using spectroscopic tools like Fourier transform IR and X-ray photoelectron spectroscopy. These rearrangements were rationalized with changes in the persistence length of DNA upon hybridization (persistence length of ss-DNA ~ 1 nm and for ds-DNA ~ 50 nm). In order to compare directly our results on DNA NAMs patches with those on DNA SAMs, we have performed experiments comparing self-assembled, high-density DNA monolayers produced following Tarlov's protocols with AFM tip-induced nanoassemblies of the same DNA sequence on the same surface. From our height measurements, we can show that a low density ($S/A = 5$) patch is 3 times higher than a maximum density SAM. Since a high density NAM is about 1.5 times as high as these lower density samples (see Figure 2) it follows that a maximum density SAM is about 4.5 times lower than a high density NAM. It is also pertinent and interesting to note that, due to molecular entanglement, that is, the existence of empty space at the interior of the SAM, the latter system is much more compressible than a nonentangled NAM.

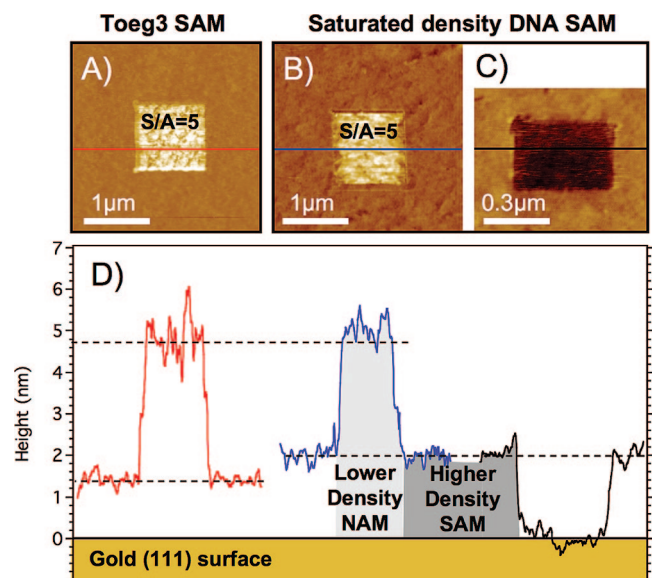


Figure 5. (A) A ssDNA NAM is grafted in low density range ($S/A = 5$) within an OEG-terminated bioresistant SAM. (B) A ssDNA NAM is grafted in low density range ($S/A = 5$) within an high density ssDNA SAM of the same molecule of the NAM. (C) A shaving of the high density DNA SAM relative to panel B is used to measure the absolute height of the DNA molecules in the SAM. (D) The red graph on the left is the height profile of the DNA NAM relative to panel A (see red lines). The absolute height of the OEG SAM is about 1.5 nm (see ref 27). The blue graph in the center is the height profile of the DNA NAM relative to panel B (see blue line). The absolute height of the DNA NAM is given by the sum of the relative height between the DNA NAM and the DNA SAM in panel B (see blue line) and the absolute height of the DNA SAM relative to panel C that is reported with the green graph on the right (see green line). Reasonably, the height of the low density NAMs grafted in the OEG terminated SAM (see panel A) and in the high density DNA SAM (see panel B) are the same while, surprisingly, although the molecular density of the NAM has to be lower than in the SAM, the height of a “low” density NAM is found to be about 3 times higher than the one of the high density SAM.

Looking at the future, we can be confident, along with Liu and co-workers, about the possibility of fabricating DNA nanoarrays of unprecedented sensitivity, but by controlling probe molecule packing and/or nonentanglement we can be confident about the quantitative aspects of the analysis of gene expression profiling including, eventually, PCR free single cell analysis. Our method, being based on height and elasticity measurements before and after hybridization, requires no labeling of the target molecules with this being no minor advantage if we are thinking about its widespread use, for instance, for screening purposes.

Acknowledgment. The authors are grateful for stimulating discussions about DNA nanoarrays with Professor Michele Morgante, Professor Francesco Stellacci, and Professor Giorgio Stanta, and for the precious contribution of Rosa

Poetes, Arum Amy Yu, and Martina Dell’Angela for the optimization of the DNA nanografting procedure. The experiments were carried out in the Sissa-ILT/Elettra Laboratory at the Elettra Synchrotron Radiation Facility in Trieste, Italy, and partially supported by the Ministero dell’Università e della Ricerca PRIN 2006020543. C.G. thanks the Alexander-von-Humboldt Foundation for a Feodor-Lynen post-doctoral fellowship.

Supporting Information Available: Experimental procedure. This material is available free of charge via the Internet at <http://pubs.acs.org>.

References

- (1) Todd, R.; Margolin, D. H. *Trends Mol. Med.* **2002**, *8*, 254–257.
- (2) Nygaard, V.; Hovig, E. *Nucleic Acids Res.* **2006**, *34* (3), 996–1014.
- (3) Mischel, P. S.; Cloughesy, T. F.; Nelson, S. F. *Nat. Rev. Neurosci.* **2004**, *5* (10), 782–792.
- (4) Hesse, J.; Jacak, J.; Kasper, M.; Regl, G.; Eichberger, T.; Winklmayr, M.; Aberger, F.; Sonnleitner, M.; Schlapak, R.; Howorka, S.; Muresan, L.; Frischauf, A.-M.; Schutz, G. J. *Genome Res.* **2006**, *16* (8), 1041–1045.
- (5) Galvin, J. E.; Ginsberg, S. D. *Ageing Res. Rev.* **2005**, *4* (4), 529–547.
- (6) Evans, S. J.; Watson, S. J.; Akil, H. *Integr. Comp. Biol.* **2003**, *43* (6), 780–785.
- (7) Draghici, S.; Khatri, P.; Eklund, A. C.; Szallasi, Z. *Trends Genet.* **2006**, *22* (2), 101–109.
- (8) Reed, J.; Mishra, B.; Pittenger, B.; Magonov, S.; Troke, J.; Teittel, M. A.; Gimzewski, J. K. *Nanotechnology* **2007**, *18* (4), 044032.
- (9) Drummond, T. G.; Hill, M. G.; Barton, J. K. *Nat. Biotechnol.* **2003**, *21* (10), 1192–1199.
- (10) Wang, J.; Bard, A. J. *Anal. Chem.* **2001**, *73* (10), 2207–2212.
- (11) Fang, S.; Lee, H. J.; Wark, A. W.; Corn, R. M. *J. Am. Chem. Soc.* **2006**, *128* (43), 14044–14046.
- (12) Marta Bally, M. H. *Surf. Interface Anal.* **2006**, *38*, 1442–1458.
- (13) Wang, J. *Nucleic Acids Res.* **2000**, *28* (16), 3011–3016.
- (14) Ambros, V. *Nature* **2004**, *431* (7006), 350–355.
- (15) Barad, O.; Meiri, E.; Avniel, A.; Aharonov, R.; Barzilai, A.; Bentwich, I.; Einav, U.; Gilad, S.; Hurban, P.; Karov, Y.; Lobenhofer, E. K.; Sharon, E.; Shibolet, Y. M.; Shtutman, M.; Bentwich, Z.; Einat, P. *Genome Res.* **2004**, *14* (12), 2486–2494.
- (16) Herne, T. M.; Tarlov, M. J. *J. Am. Chem. Soc.* **1997**, *119* (38), 8916–8920.
- (17) Peterlinz, K. A.; Georgiadis, R. M.; Herne, T. M.; Tarlov, M. J. *J. Am. Chem. Soc.* **1997**, *119* (14), 3401–3402.
- (18) Peterson, A. W.; Heaton, R. J.; Georgiadis, R. M. *Nucleic Acids Res.* **2001**, *29* (24), 5163–5168.
- (19) Petrovykh, D. Y.; Kimura-Suda, H.; Whitman, L. J.; Tarlov, M. J. *J. Am. Chem. Soc.* **2003**, *125* (17), 5219–5226.
- (20) Steel, A. B.; Levicky, R. L.; Herne, T. M.; Tarlov, M. J. *Biophys. J.* **2000**, *79* (2), 975–981.
- (21) Liu, M.; Amro, N. A.; Chow, C. S.; Liu, G. Y. *Nano Lett.* **2002**, *2* (8), 863–867.
- (22) Liu, M.; Liu, G. Y. *Langmuir* **2005**, *21* (5), 1972–1978.
- (23) Xu, S.; Liu, G. Y. *Langmuir* **1997**, *13* (2), 127–129.
- (24) Liu, G. Y.; Xu, S.; Qian, Y. *Acc. Chem. Res.* **2000**, *33* (7), 457–466.
- (25) Kramer, S.; Fuierer, R. R.; Gorman, C. B. *Chem. Rev.* **2003**, *103* (11), 4367–4418.
- (26) Ryu, S.; Schatz, G. C. *J. Am. Chem. Soc.* **2006**, *128* (35), 11563–11573.
- (27) Hu, Y. Ph.D. Thesis, Princeton University, Princeton, NJ, 2005.
- (28) Grunwald, C. 2008, unpublished results.
- (29) Sinensky, A. K.; Belcher, A. M. *Nat. Nanotechnol.* **2007**, *2* (10), 653–659.

NL802722K